PHYSICAL REVIEW B **93**, 180502(R) (2016)

Nematicity and in-plane anisotropy of superconductivity in β-FeSe detected by ^{77}Se nuclear magnetic resonance

S.-H. Baek,[1,*] D. V. Efremov,[1] J. M. Ok,[2] J. S. Kim,[2] Jeroen van den Brink,[1,3] and B. Büchner[1,3]

[1]*IFW Dresden, Helmholtzstrasse 20, 01069 Dresden, Germany*

[2]*Department of Physics, Pohang University of Science and Technology, Pohang 790-784, Korea*

[3]*Department of Physics, Technische Universität Dresden, 01062 Dresden, Germany*

(Received 21 October 2015; revised manuscript received 25 March 2016; published 10 May 2016)

The recent study of ^{77}Se nuclear magnetic resonance (NMR) in a β-FeSe single crystal proposed that ferro-orbital order breaks the 90° C_4 rotational symmetry, driving nematic ordering. Here, we report an NMR study of the impact of small strains generated by gluing on nematic state and spin fluctuations. We observe that the local strains strongly affect the nematic transition, considerably enhancing its onset temperature. On the contrary, no effect on low-energy spin fluctuations was found. Furthermore we investigate the interplay of the nematic phase and superconductivity. Our study demonstrates that the twinned nematic domains respond unequivalently to superconductivity, evidencing the twofold C_2 symmetry of superconductivity in this material. The obtained results are well understood in terms of the proposed ferro-orbital order.

DOI: 10.1103/PhysRevB.93.180502

Many experiments have established the existence of nematic order—a state that spontaneously breaks the rotational symmetry while time-reversal invariance is preserved—in Fe-based superconductors (FeSCs) [1–8]. Although whether spin or orbital degrees of freedom drive the nematic order is still under debate [9–15], it is widely believed that a nematic instability is an important characteristic of the normal state from which superconductivity emerges. Therefore establishing the mechanism of the nematic order will help to elucidate the Cooper pair glue in FeSCs.

In most FeSCs, the nematic state arises in the vicinity of a spin-density wave state. The temperature (T) interval separating them is small. As a result the strong interaction of various degrees of freedom hides the nature of the nematic order. The only exception is β-FeSe which has a PbO-type crystal structure. The nematic order occurs at $T_{\rm nem} \approx 91$ K, and at a lower temperature of $T_c \approx 9$ K SC sets in. The absence of static magnetism in the whole interval of temperature together with its simple structure [16] make β-FeSe the primary object for investigation of nematicity and its interplay with SC [14,17–26]. To other spectacular properties of β-FeSe belongs the dramatic increase in T_c under pressure [27,28] or by growing monolayer films on substrates [29–31].

The band structure of β-FeSe is typical for FeSC [32,33]. The low energy is given by two hole bands around the Γ point and two electron bands around the M point. The nesting between the electron and the hole bands advocates strong spin fluctuations (SFs) at low T which indeed were observed in nuclear magnetic resonance (NMR) and neutron studies at $T \ll T_{\rm nem}$. However no enhancement of SFs was found close to the nematic transition. It led to the suggestion that nematic state in β-FeSe is driven by orbital degrees of freedom [34–37].

In this Rapid Communication, we report the investigations of nematic order in the normal and superconducting states of β-FeSe. We show that gluing the sample introduces random local strains (defects) and significantly smears out the otherwise sharp nematic transition resulting in the enhanced onset of nematic ordering. In contrast, it appears that low-energy SFs are essentially unaffected by the strain. Furthermore, we demonstrate that the twofold C_2 symmetry of SC in this material is the consequence of the interplay between orbital and superconducting order parameters.

The ^{77}Se NMR measurements were carried out in a β-FeSe single crystal from the same batch as the one measured in the previous study [35] at an external field ($\mu_0 H$) of 9 T and in the T range of 4.2–180 K. The sample was mounted to a single-axis goniometer for the exact alignment along **H** within the a-c plane of the crystal. The ^{77}Se NMR spectra were obtained by a standard spin-echo technique, and the ^{77}Se spin-lattice relaxation rate T_1^{-1} was measured using a saturation method by fitting the recovery of the nuclear magnetization $M(t)$ to a single exponential function $1 - M(t)/M(\infty) = A\exp(-t/T_1)$, where A is a fitting parameter that is ideally unity. In this Rapid Communication, we glued the sample inside the NMR coil using a small amount of diluted GE varnish not only for the better and stable alignment of the sample, but also for examining a possible effect of gluing on nematicity. The motivation is that while using a glue on samples is unavoidable in many bulk measurements, it is unknown whether there are nontrivial effects of random strains that could be introduced by gluing.

Figure 1(a) shows ^{77}Se NMR spectra as a function of T at $\mu_0 H = 9$ T applied along the crystallographic a axis. The ^{77}Se line splits into the two lines $\ell_{1,2}$ below $T_{\rm nem} \sim 91$ K, which is consistent with the previous results [35]. In Ref. [35], it was established that the splitting of the ^{77}Se line is much larger than one could expect from the small orthorhombic distortion. In order to further demonstrate that the split ^{77}Se NMR lines truly represent the nematic order parameter, we measured the ^{77}Se spectrum at a fixed T of 60 K as a function of angle θ between the **H** and the c directions by rotating the sample with respect to **H** from a toward c on the a-c plane. The resultant angle dependence of the ℓ_1-ℓ_2 spectrum and their Knight shifts $\mathcal{K}$ are shown in Figs. 1(b) and 1(c), respectively. $\mathcal{K}$'s of both ℓ_1 and ℓ_2 decrease with decreasing θ following a cosine function of θ and smoothly merge into a single line when $H \parallel c$. As a result, the difference of the Knight shifts $\Delta\mathcal{K}_{\parallel a}$ [see the inset

*sbaek.fu@gmail.com

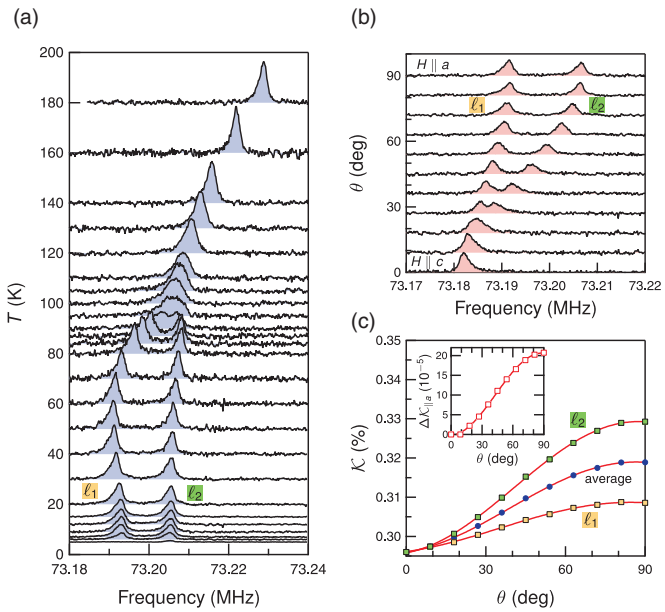

FIG. 1. (a) The ^{77}Se NMR spectra for a β-FeSe single crystal measured at $\mu_0 H = 9$ T applied along the a axis as a function of T. The splitting of the ^{77}Se line into two (labeled ℓ_1 and ℓ_2) was observed near $T_{\rm nem} \sim 91$ K. (b) A ^{77}Se spectrum measured at 60 K as a function of angle θ between the **H** and the c directions. (c) Knight shifts of ℓ_1-ℓ_2 lines and $\Delta\mathcal{K}_{\|a}$ (see the inset) as a function of θ follow a simple cosine function (solid lines) as expected for a nematic order parameter.

of Fig. 1(c)] is perfectly described by a cosine function of θ (solid line). This unambiguously verifies that $\Delta\mathcal{K}_{\|a}$ indeed reflects the nematic order parameter, which is anticipated to obey such a sinusoidal angle dependence.

Although the T evolution of the ^{77}Se NMR spectrum is very similar to the results obtained in the sample that was not glued [35], it turns out that the full width at half maximum of NMR lines are two to three times broader. Since both the current and the previous NMR studies have been carried out on the crystals from the same batch under the identical experimental setup and conditions, the inhomogeneous NMR line broadening is attributed to local strains introduced by gluing the sample. In addition to the inhomogeneous broadening of the ^{77}Se lines, we find that the nematic transition is not as sharp as in the previous study. Namely, the line splitting does not disappear immediately above the nematic transition temperature $T_{\rm nem} = 91$ K but persists up to higher T. Indeed, Figs. 2(a) and 2(b) indicate that the ℓ_1 and ℓ_2 lines start to split at $T^* \sim 120$ K that is significantly higher than $T_{\rm nem}$. In this regard, we refer to the sample that was not glued as strain free. Since in the range of $T_{\rm nem} < T < T^*$ the material remains in the tetragonal symmetry in bulk, the persisting NMR line splitting above $T_{\rm nem}$ indicates that the 90° rotational symmetry should be broken only near local strains. The reason may be the emergence of the local nematic order $\psi(\mathbf{r})$, which exists only locally as a form of small domains without affecting the bulk tetragonal phase of the crystal, by coupling to the local uniaxial strains caused by the gluing. In this case, the broad NMR line between $T_{\rm nem} \leqslant T \leqslant T^*$, which is not well resolved, may consist of three lines: the split ℓ_1-ℓ_2 lines from the regions near strains and the unsplit line from the tetragonal region away from strains.

A description of the T dependence of the nematic order parameter ψ can be done in the frame of the Landau theory. The free energy in the presence of an external uniaxial stress σ has the following form:

$$\Delta F = \alpha(T - T_{\rm nem})\psi^2 + \frac{b}{2}\psi^4 - \lambda\sigma\psi. \qquad (1)$$

For simplicity we neglect the spatial variation of the nematic order parameter assuming that the size of the domains is large. The effective coupling constant λ is a T-independent function of the shear modulus $C_{66,0}$ that can be obtained by integrating out the structural degree of freedom from the

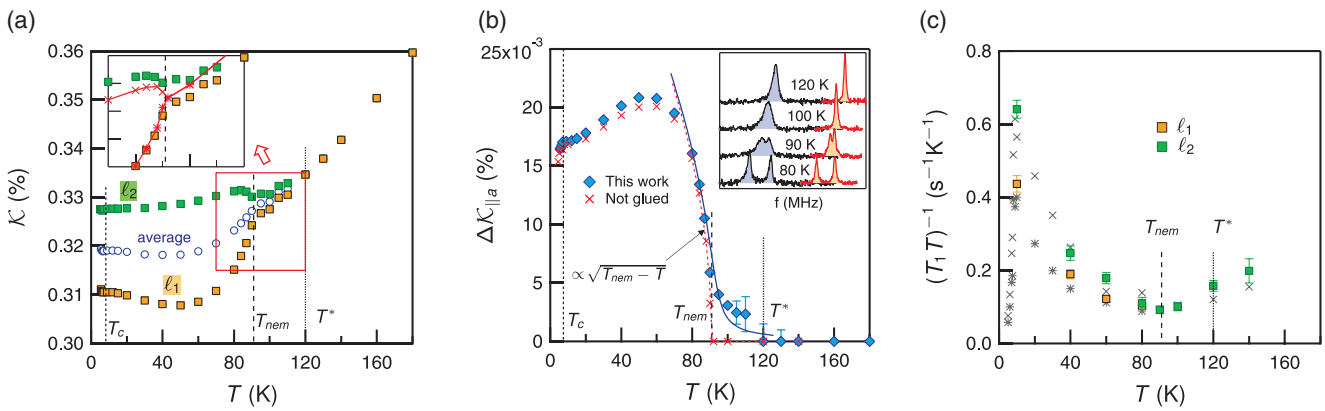

FIG. 2. (a) and (b) Temperature dependence of the ^{77}Se NMR Knight shift $\mathcal{K}$ and the ℓ_1-ℓ_2 splitting $\Delta\mathcal{K}_{\|a}$, respectively. The comparison with the results in Ref. [35] which were rescaled by 1.15 reveals that the actual splitting occurs at $T^* \sim 120$ K significantly higher than $T_{\rm nem} = 91$ K. $\Delta\mathcal{K}_{\|a}$ becomes proportional to $\sqrt{T_{\rm nem} - T}$ below $T_{\rm nem}$ indicating that $T_{\rm nem}$ is the true nematic transition temperature. The solid and dashed curves in (b) are theoretical calculations (see the text). The inset in (a) shows an enlargement of the region denoted by the red rectangle to compare with the sharp splitting observed in a "strain-free" sample [35]. The raw ^{77}Se spectra from the current Rapid Communication (left) and those from Ref. [35] (right) in selected temperatures near $T_{\rm nem}$ are compared in the inset of (b). (c) T dependence of the spin-lattice relaxation rate divided by T $(T_1T)^{-1}$ near $T_{\rm nem}$. The asterisk (∗) and cross (×) symbols in gray represent the data of ℓ_1 and ℓ_2, respectively, measured without gluing the sample [35].

Landau functional [38]. The linear coupling of ψ to σ leads to the induced nematicity seen in the range of $T_{\rm nem} \leqslant T \leqslant T^*$. For $T < T_{\rm nem}$, the contribution of σ to ΔF is negligible. Therefore the T dependence of ψ is not affected by local strains due to gluing as shown in Fig. 2(b). The solution $\psi(T)$ minimizing the Landau functional Eq. (1) is continuous. In the case of a structure with two types of domains with strain and without strain, the splitting seen for $T > T_{\rm nem}$ is mainly given by the domains with strain, whereas for $T < T_{\rm nem}$ both cases give the same NMR line splitting. The solutions of Eq. (1) are given as the solid and dashed curves in Fig. 2(b) where the values of the parameters are the same for both cases, but the solid curve corresponds to 20% of the sample volume being under the stress. It is interesting to note that in $BaFe_2(As_{1-x}P_x)_2$ a similar nematic onset was observed in magnetic torque measurements by Kasahara *et al.* [39]. For β-FeSe we have the advantage to be able to compare strained and unstrained samples and observe that at a higher T the onset of the nematic ordering is absent in pristine strain-free crystals, see Fig. 2(b), and only present in glued crystals, which are affected by strain. In β-FeSe the transition at 91 K is therefore of nematic nature and does not share the metanematic origin that has been assigned to it in $BaFe_2(As_{1-x}P_x)_2$.

Having established that the local strains significantly enhance local nematicity, the question arises whether antiferromagnetic SFs are influenced by them. To check this, we measured the spin-lattice relaxation rate divided by T $(T_1T)^{-1}$ which probes low-energy SFs. As shown in Fig. 2(c), $(T_1T)^{-1}$ is almost intact near $T_{\rm nem}$ and reveals the same behavior as observed in the strain-free sample [35]. This suggests that the low-energy magnetic excitations are hardly affected by the enhanced nematicity.

In parallel to the enhanced onset of nematicity, one can notice that the nematic order parameter $\Delta\mathcal{K}_{\|a}$ as shown in Fig. 2(b) where the previous data were rescaled by 1.15 are enhanced compared to the previous data. A possible origin is a better alignment of **H** along the a axis in the present Rapid Communication, but it could be also local strains that enhance the nematicity. Regardless, an important observation is that $\Delta\mathcal{K}_{\|a}$ reveals an identical T dependence with that in Ref. [35]. They form a maximum near 60 K and decrease with decreasing T. At the same time the average of the Knight shifts $\mathcal{K}_{\rm av} = \mathcal{K}_a + \mathcal{K}_b$ and $\mathcal{K}_{\|c}$ show no change with T below 60 K. The increase in the splitting $\Delta\mathcal{K}_{\|a}$ in the T interval between $T_{\rm nem}$ and 60 K can be certainly attributed to the increase in the anisotropy of hyperfine couplings $A^{\rm hf}_{xx} - A^{\rm hf}_{xx} \propto \psi$ and the spin susceptibilities $(\chi_{xx} - \chi_{yy}) \propto \psi$ as $\Delta\mathcal{K}_{\|a}$ depends on both of these values $\Delta\mathcal{K}_{\|a} = 1/2(A^{\rm hf}_{xx} + A^{\rm hf}_{yy})(\chi_{xx} - \chi_{yy}) + 1/2(A^{\rm hf}_{xx} - A^{\rm hf}_{yy})(\chi_{xx} + \chi_{yy})$. The decrease in $\Delta\mathcal{K}_{\|a}$ with no T change in $\mathcal{K}_{\|c} = A^{\rm hf}_c\chi_{zz}$ and the average $\mathcal{K}_{\rm av} = 1/2(A^{\rm hf}_{xx} + A^{\rm hf}_{yy})(\chi_{xx} + \chi_{yy}) + 1/2(A^{\rm hf}_{xx} - A^{\rm hf}_{yy})(\chi_{xx} - \chi_{yy})$ below 60 K is a more subtle question. It cannot be explained by the nonanalytic contributions to the spin susceptibility in two-dimensional Fermi liquid as they would also give a linear in T contribution to $\mathcal{K}_{\|c}$ and $\mathcal{K}_{\rm av}$. Another interesting observation is that the decrease in $\Delta\mathcal{K}_{\|a}$ is accompanied by the increase in the low-energy SFs seen in the spin-lattice relaxation rate $(T_1T)^{-1}$ [see Fig. 2(c)]. This suggests, contrary to the scenario of the spin nematic [12], that the increase in SFs results in the suppression of the nematic order. That is, SFs alone may be insufficient to drive nematic order in β-FeSe.

Now we focus on the NMR data in the superconducting state. In the previous NMR study, we have shown that $\Delta\mathcal{K}_{\|a}$ abruptly decreases just below T_c. A similar anomalous change in $\Delta\mathcal{K}_{\|a}$ below T_c was also observed as shown in Fig. 2(b), but it appears that the drop of $\Delta\mathcal{K}_{\|a}$ is much less pronounced than in the previous result. This is in line with the consideration that nematicity is strengthened due to gluing, rendering it more robust against the competition of the superconducting order parameter [35,40]. Clearly one expects that the nematic ordering, which appears at a much higher T than SC, is only marginally affected by SC, but *vice versa* that SC is much more strongly affected by the presence of already preformed nematic order that breaks the in-plane symmetry. The latter we indeed observe as well and is revealed by measurement of the T dependence of intensities of the ℓ_1 and ℓ_2 lines below T_c.

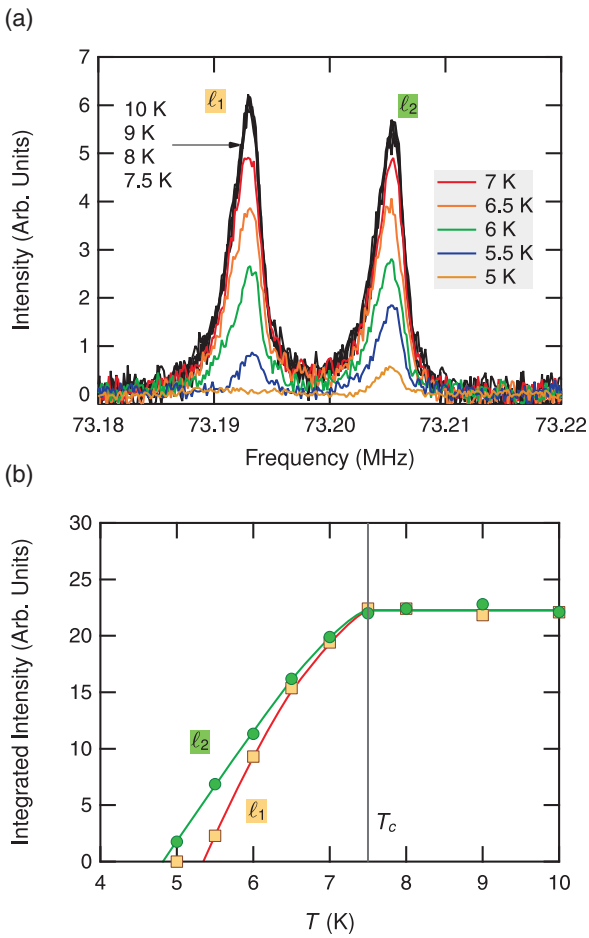

FIG. 3. (a) Temperature dependence of the split ^{77}Se spectrum measured at low T for $\mu_0H = 9$ T applied along the a axis. Both ℓ_1 and ℓ_2 lines start to lose their intensities below 7.5 K, but the intensity of ℓ_1 decreases faster than that of ℓ_2 with decreasing T. A Boltzmann correction was performed by multiplying T to each spectrum. (b) Integrated NMR signal intensities of ℓ_1 and ℓ_2, respectively, as a function of T. The ℓ_1 and ℓ_2 intensities are normalized at 10 K. The different T dependence of the ℓ_1 and ℓ_2 signal intensities is clearly revealed, whereas $T_c \sim 7.5$ K is identical for both NMR lines. The solid lines are guides to the eyes.

The ℓ_1 and ℓ_2 lines represent the twinned nematic domains, and their T dependence below T_c is presented in Fig. 2(a). To begin with, it should be noted that ℓ_1 has a slightly bigger intensity than ℓ_2 in the normal state above 7.5 K, indicating that one of the twinned nematic domains coincidentally has larger volume than the other. Although the two NMR lines have an unchanged signal intensity with T in the normal state, we observed that just below T_c they lose the signal intensity rapidly with decreasing T. In general, the loss of the NMR signal intensity $I_{\rm NMR}$ in the SC state takes place due to diamagnetism of SC. The penetration of the radio-frequency (rf) pulses into the bulk sample is hampered by supercurrents generated on the surface and, as a consequence, the total number of nuclei that could be irradiated by the rf pulses (thus $I_{\rm NMR}$) is reduced accordingly. Therefore, one can view that $I_{\rm NMR}$ is proportional to the SC penetration depth λ, although it is difficult to quantify $I_{\rm NMR}$ in terms of λ because there are also many different contributions to $I_{\rm NMR}$, such as the inhomogeneous field distribution due to the presence of vortices, vortex dynamics, and the Q factor of the NMR circuit. However, these factors are the same for the two nematic domains that are present in the sample—these domains only differ in their relative orientation with respect to the in-plane magnetic field, which is rotated by exactly 90°.

Strikingly, Fig. 3(a) reveals that at 5 K ℓ_1 is almost quenched whereas ℓ_2 is visible, in sharp contrast with the fact that ℓ_1 has a bigger intensity than ℓ_2 above T_c. This means that ℓ_1 is losing intensity faster than ℓ_2 with lowering T in the SC state. Indeed, as shown in Fig. 3(b), the integrated signal intensity as a function of T reveals the distinctly different T dependence of ℓ_1 and ℓ_2. Since the split ℓ_1-ℓ_2 lines represent the twinned domains whose nematicity are parallel and perpendicular, respectively, to **H**, without further analysis, we already conclude that the SC response of the two domains is inequivalent, indicating that $\lambda_a \neq \lambda_b$. Actually in the clean limit at low T the anisotropy in penetration depth is associated with the anisotropy in the velocities due to the nematic phase as $\lambda_a^{-2}/\lambda_b^{-2} \rightarrow \langle v_a^2\rangle/\langle v_b^2\rangle$ [41]. This implies that the broken in-plane symmetry of SC is a natural consequence of the elongated Fermi surface caused by orbital ordering.

This tetragonal symmetry breaking of λ is indeed consistent with the highly elongated vortex core along the a axis observed by scanning tunneling microscopy in FeSe films on a SiC substrate [4]. The twofold symmetry of the vortex core state can be understood by the difference between SC coherence length ξ along the a and b directions, being attributed to the strong impact of the nematic order on SC [42,43].

In conclusion, we presented a NMR study of a β-FeSe single crystal under small strain generated by gluing. We found that the local strains considerably affect the nematic order, whereas no effect on low-energy SFs was found. These results suggest that nematicity in β-FeSe is not driven by SFs, supporting the orbital ordering picture. The unusual in-plane anisotropy of the penetration depth λ manifests the twofold symmetry breaking of SC due to orbital ordering.

We thank H. Kontani, T. Boothroyd, B. M. Andersen, and R. Fernandes for useful discussions. This work has been supported by the Deutsche Forschungsgemeinschaft (Germany) via DFG Research Grant No. BA 4927/1-3 and the Priority Program SPP 1458. The work at POSTECH was supported by the NRF through SRC (Grant No. 2011-0030785) and the Max Planck POSTECH/KOREA Research Initiative (Grant No. 2011-0031558) programs and by IBS (Grant No. IBSR014-D1-2014-a02) through the Center for Artificial Low Dimensional Electronic Systems.

[1] T.-M. Chuang, M. P. Allan, J. Lee, Y. Xie, N. Ni, S. L. Bud'ko, G. S. Boebinger, P. C. Canfield, and J. C. Davis, Nematic electronic structure in the "Parent" state of the iron-based superconductor $Ca(Fe_{1-x}Co_x)_2As_2$, Science **327**, 181 (2010).

[2] M. A. Tanatar, E. C. Blomberg, A. Kreyssig, M. G. Kim, N. Ni, A. Thaler, S. L. Bud'ko, P. C. Canfield, A. I. Goldman, I. I. Mazin, and R. Prozorov, Uniaxial-strain mechanical detwinning of $CaFe_2As_2$ and $BaFe_2As_2$ crystals: Optical and transport study, Phys. Rev. B **81**, 184508 (2010).

[3] J. J. Ying, X. F. Wang, T. Wu, Z. J. Xiang, R. H. Liu, Y. J. Yan, A. F. Wang, M. Zhang, G. J. Ye, P. Cheng, J. P. Hu, and X. H. Chen, Measurements of the Anisotropic In-Plane Resistivity of Underdoped Feas-Based Pnictide Superconductors, Phys. Rev. Lett. **107**, 067001 (2011).

[4] C.-L. Song, Y.-L. Wang, P. Cheng, Y.-P. Jiang, W. Li, T. Zhang, Z. Li, K. He, L. Wang, J.-F. Jia, H.-H. Hung, C. Wu, X. Ma, X. Chen, and Q.-K. Xue, Direct observation of nodes and twofold symmetry in FeSe superconductor, Science **332**, 1410 (2011).

[5] M. Yi, D. Lu, J.-H. Chu, J. G. Analytis, A. P. Sorini, A. F. Kemper, B. Moritz, S.-K. Mo, R. G. Moore, M. Hashimoto, W.-S. Lee, Z. Hussain, T. P. Devereaux, I. R. Fisher, and Z.-X. Shen, Symmetry-breaking orbital anisotropy observed for detwinned $Ba(Fe_{1-x}Co_x)_2As_2$ above the spin density wave transition, Proc. Natl. Acad. Sci. USA **108**, 6878 (2011).

[6] J.-H. Chu, H.-H. Kuo, J. G. Analytis, and I. R. Fisher, Divergent nematic susceptibility in an iron arsenide superconductor, Science **337**, 710 (2012).

[7] E. P. Rosenthal, E. F. Andrade, C. J. Arguello, R. M. Fernandes, L. Y. Xing, X. C. Wang, C. Q. Jin, A. J. Millis, and A. N. Pasupathy, Visualization of electron nematicity and unidirectional antiferroic fluctuations at high temperatures in NaFeAs, Nat. Phys. **10**, 225 (2014).

[8] T. Iye, M.-H. Julien, H. Mayaffre, M. Horvatić, C. Berthier, K. Ishida, H. Ikeda, S. Kasahara, T. Shibauchi, and Y. Matsuda, Emergence of orbital nematicity in the tetragonal phase of $BaFe_2(As_{1-x}P_x)_2$, J. Phys. Soc. Jpn. **84**, 043705 (2015).

[9] W. Lv, J. Wu, and P. Phillips, Orbital ordering induces structural phase transition and the resistivity anomaly in iron pnictides, Phys. Rev. B **80**, 224506 (2009).

[10] W. Lv, F. Krüger, and P. Phillips, Orbital ordering and unfrustrated $(\pi,0)$ magnetism from degenerate double exchange in the iron pnictides, Phys. Rev. B **82**, 045125 (2010).

[11] S. Liang, A. Moreo, and E. Dagotto, Nematic State of Pnictides Stabilized by Interplay between Spin, Orbital, and

Lattice Degrees of Freedom, Phys. Rev. Lett. **111**, 047004 (2013).

[12] R. M. Fernandes, A. V. Chubukov, and J. Schmalian, What drives nematic order in iron-based superconductors?, Nat. Phys. **10**, 97 (2014).

[13] H. Kontani and Y. Yamakawa, Linear Response Theory for Shear Modulus C_{66} and Raman Quadrupole Susceptibility: Evidence for Nematic Orbital Fluctuations in Fe-based Superconductors, Phys. Rev. Lett. **113**, 047001 (2014).

[14] A. V. Chubukov, R. M. Fernandes, and J. Schmalian, Origin of nematic order in FeSe, Phys. Rev. B **91**, 201105 (2015).

[15] R. Yu and Q. Si, Antiferroquadrupolar and Ising-Nematic Orders of a Frustrated Bilinear-Biquadratic Heisenberg Model and Implications for the Magnetism of FeSe, Phys. Rev. Lett. **115**, 116401 (2015).

[16] F.-C. Hsu, J.-Y. Luo, K.-W. Yeh, T.-K. Chen, T.-W. Huang, P. M. Wu, Y.-C. Lee, Y.-L. Huang, Y.-Y. Chu, D.-C. Yan, and M.-K. Wu, Superconductivity in the PbO-type structure α-FeSe, Proc. Natl. Acad. Sci. USA **105**, 14262 (2008).

[17] K. K. Huynh, Y. Tanabe, T. Urata, H. Oguro, S. Heguri, K. Watanabe, and K. Tanigaki, Electric transport of a single-crystal iron chalcogenide FeSe superconductor: Evidence of symmetry-breakdown nematicity and additional ultrafast Dirac cone-like carriers, Phys. Rev. B **90**, 144516 (2014).

[18] K. Nakayama, Y. Miyata, G. N. Phan, T. Sato, Y. Tanabe, T. Urata, K. Tanigaki, and T. Takahashi, Reconstruction of Band Structure Induced by Electronic Nematicity in an FeSe Superconductor, Phys. Rev. Lett. **113**, 237001 (2014).

[19] T. Shimojima, Y. Suzuki, T. Sonobe, A. Nakamura, M. Sakano, J. Omachi, K. Yoshioka, M. Kuwata-Gonokami, K. Ono, H. Kumigashira, A. E. Böhmer, F. Hardy, T. Wolf, C. Meingast, H. v. Löhneysen, H. Ikeda, and K. Ishizaka, Lifting of xz/yz orbital degeneracy at the structural transition in detwinned FeSe, Phys. Rev. B **90**, 121111 (2014).

[20] A. E. Böhmer, T. Arai, F. Hardy, T. Hattori, T. Iye, T. Wolf, H. v. Löhneysen, K. Ishida, and C. Meingast, Origin of the Tetragonal-to-Orthorhombic Phase Transition in FeSe: A Combined Thermodynamic and NMR Study of Nematicity, Phys. Rev. Lett. **114**, 027001 (2015).

[21] M. C. Rahn, R. A. Ewings, S. J. Sedlmaier, S. J. Clarke, and A. T. Boothroyd, Strong $(\pi,0)$ spin fluctuations in β-FeSe observed by neutron spectroscopy, Phys. Rev. B **91**, 180501 (2015).

[22] Q. Wang, Y. Shen, B. Pan, Y. Hao, M. Ma, F. Zhou, P. Steffens, K. Schmalzl, T. R. Forrest, M. Abdel-Hafiez, X. Chen, D. A. Chareev, A. N. Vasiliev, P. Bourges, Y. Sidis, H. Cao, and J. Zhao, Strong interplay between stripe spin fluctuations, nematicity and superconductivity in FeSe, Nature Mater. **15**, 159 (2016).

[23] M. D. Watson, T. K. Kim, A. A. Haghighirad, N. R. Davies, A. McCollam, A. Narayanan, S. F. Blake, Y. L. Chen, S. Ghannadzadeh, A. J. Schofield, M. Hoesch, C. Meingast, T. Wolf, and A. I. Coldea, Emergence of the nematic electronic state in FeSe, Phys. Rev. B **91**, 155106 (2015).

[24] S. Mukherjee, A. Kreisel, P. J. Hirschfeld, and B. M. Andersen, Model of Electronic Structure and Superconductivity in Orbitally Ordered FeSe, Phys. Rev. Lett. **115**, 026402 (2015).

[25] J. K. Glasbrenner, I. I. Mazin, H. O. Jeschke, P. J. Hirschfeld, R. M. Fernandes, and R. Valenti, Effect of magnetic frustration on nematicity and superconductivity in iron chalcogenides, Nat. Phys. **11**, 953 (2015).

[26] S. Rößler, C. Koz, L. Jiao, U. K. Rößler, F. Steglich, U. Schwarz, and S. Wirth, Emergence of an incipient ordering mode in FeSe, Phys. Rev. B **92**, 060505 (2015).

[27] S. Margadonna, Y. Takabayashi, Y. Ohishi, Y. Mizuguchi, Y. Takano, T. Kagayama, T. Nakagawa, M. Takata, and K. Prassides, Pressure evolution of the low-temperature crystal structure and bonding of the superconductor FeSe ($T_c = 37$ K), Phys. Rev. B **80**, 064506 (2009).

[28] S. Medvedev, T. M. McQueen, I. A. Troyan, T. Palasyuk, M. I. Eremets, R. J. Cava, S. Naghavi, F. Casper, V. Ksenofontov, G. Wortmann, and C. Felser, Electronic and magnetic phase diagram of β-$Fe_{1.01}Se$ with superconductivity at 36.7 K under pressure, Nature Mater. **8**, 630 (2009).

[29] Y.-Y. Xiang, F. Wang, D. Wang, Q.-H. Wang, and D.-H. Lee, High-temperature superconductivity at the FeSe/$SrTiO_3$ interface, Phys. Rev. B **86**, 134508 (2012).

[30] S. He, J. He, W. Zhang, L. Zhao, D. Liu, X. Liu, D. Mou, Y.-B. Ou, Q.-Y. Wang, Z. Li, L. Wang, Y. Peng, Y. Liu, C. Chen, L. Yu, G. Liu, X. Dong, J. Zhang, C. Chen, Z. Xu, X. Chen, X. Ma, Q. Xue, and X. J. Zhou, Phase diagram and electronic indication of high-temperature superconductivity at 65 K in single-layer FeSe films, Nature Mater. **12**, 605 (2013).

[31] J.-F. Ge, Z.-L. Liu, C. Liu, C.-L. Gao, D. Qian, Q.-K. Xue, Y. Liu, and J.-F. Jia, Superconductivity above 100 K in single-layer FeSe films on doped $SrTiO_3$, Nature Mater. **14**, 285 (2015).

[32] J. Maletz, V. B. Zabolotnyy, D. V. Evtushinsky, S. Thirupathaiah, A. U. B. Wolter, L. Harnagea, A. N. Yaresko, A. N. Vasiliev, D. A. Chareev, A. E. Böhmer, F. Hardy, T. Wolf, C. Meingast, E. D. L. Rienks, B. Büchner, and S. V. Borisenko, Unusual band renormalization in the simplest iron-based superconductor $FeSe_{1-x}$, Phys. Rev. B **89**, 220506 (2014).

[33] P. Zhang, T. Qian, P. Richard, X. P. Wang, H. Miao, B. Q. Lv, B. B. Fu, T. Wolf, C. Meingast, X. X. Wu, Z. Q. Wang, J. P. Hu, and H. Ding, Observation of two distinct d_{xz}/d_{yz} band splittings in FeSe, Phys. Rev. B **91**, 214503 (2015).

[34] Y.-C. Wen, K.-J. Wang, H.-H. Chang, J.-Y. Luo, C.-C. Shen, H.-L. Liu, C.-K. Sun, M.-J. Wang, and M.-K. Wu, Gap Opening and Orbital Modification of Superconducting FeSe above the Structural Distortion, Phys. Rev. Lett. **108**, 267002 (2012).

[35] S.-H. Baek, D. V. Efremov, J. M. Ok, J. S. Kim, J. van den Brink, and B. Büchner, Orbital-driven nematicity in FeSe, Nature Mater. **14**, 210 (2015).

[36] Y. Yamakawa, S. Onari, and H. Kontani, Nematicity and Magnetism in FeSe and other Families of Fe-based Superconductors, arXiv:1509.01161.

[37] S. Onari, Y. Yamakawa, and H. Kontani, Sign-reversing orbital polarization in the nematic phase of FeSe driven by Aslamazov-Larkin Processes, arXiv:1509.01172.

[38] A. E. Böhmer and C. Meingast, Electronic nematic susceptibility of iron-based superconductors, C. R. Phys. **17**, 90 (2015).

[39] S. Kasahara, H. J. Shi, K. Hashimoto, S. Tonegawa, Y. Mizukami, T. Shibauchi, K. Sugimoto, T. Fukuda, T. Terashima, Andriy H. Nevidomskyy, and Y. Matsuda, Electronic nematicity above the structural and superconducting transition in $BaFe_2(As_{1-x}P_x)_2$, Nature (London) **486**, 382 (2012).

[40] A. E. Böhmer, F. Hardy, F. Eilers, D. Ernst, P. Adelmann, P. Schweiss, T. Wolf, and C. Meingast, Lack of coupling between superconductivity and orthorhombic distortion in stoichiometric single-crystalline FeSe, Phys. Rev. B **87**, 180505 (2013).

[41] V. G. Kogan, Macroscopic anisotropy in superconductors with anisotropic gaps, Phys. Rev. B **66**, 020509 (2002).

[42] E.-G. Moon and S. Sachdev, Competition between superconductivity and nematic order: Anisotropy of superconducting coherence length, Phys. Rev. B **85**, 184511 (2012).

[43] H.-H. Hung, C.-L. Song, X. Chen, X. Ma, Q.-k. Xue, and C. Wu, Anisotropic vortex lattice structures in the FeSe superconductor, Phys. Rev. B **85**, 104510 (2012).